Subdivision Surfaces for Scattered-data Approximation

Martin Bertram and Hans Hagen

University of Kaiserslautern
Department of Computer Science
P.O. Box 3049
D-67653 Kaiserslautern
Germany
{bertram,hagen}@informatik.uni-kl.de

Keywords: multiresolution methods, scattered data, subdivision surfaces, terrain modeling, triangulation.

Abstract. We propose a modified Loop subdivision surface scheme for the approximation of scattered data in the plane. Starting with a triangulated set of scattered data with associated function values, our scheme applies linear, stationary subdivision rules resulting in a hierarchy of triangulations that converge rapidly to a smooth limit surface. The novelty of our scheme is that it applies subdivision only to the ordinates of control points, whereas the triangulated mesh in the plane is fixed. Our subdivision scheme defines locally supported, bivariate basis functions and provides multiple levels of approximation with triangles. We use our subdivision scheme for terrain modeling.

1 Introduction

Subdivision surfaces [4, 8] are widely used for modeling surfaces of arbitrary topological genus. They are defined by polygonal control meshes that are recursively refined analogously to knot insertion for B-spline surfaces [15]. This refinement process converges to smooth limit surfaces that are in many cases piecewise polynomials. The subdivision schemes by Catmull/Clark [7] and Doo/Sabin [9], for example, reproduce uniform B-Splines on regular, rectilinear meshes.

The strength of subdivision surfaces is their ability to deal with irregular meshes defining arbitrary two-manifolds. Extraordinary points, *i.e.*, surface points corresponding to vertices with other than four adjacent edges in a control mesh, are typically surrounded by an infinite number of smaller and smaller polynomial patches satisfying certain continuity constraints. Eigen-analysis of local subdivision matrices can be used to compute surface normals and to evaluate a limit surface at arbitrary parameter values [25, 23, 14].

Multiresolution modeling techniques, like wavelet transforms [26], are required for real-time visualization of large-scale data sets. Subdivision surfaces and wavelet transforms can be combined to a single, highly efficient multiresolution modeling tool [20, 24, 18, 3]. Subdivision-surface wavelets with finite filters have been constructed for compression and multiresolution representation of functions defined on planar tessellations and surfaces of arbitrary topology like isosurfaces [1–3]. Related multiresolution methods [12, 17] have been designed for completely irregular triangulated surfaces

without subdivision connectivity. Wavelets and subdivision techniques are also successfully being applied to computational fluid dynamics (CFD) and flow visualization problems [27, 21, 6].

Despite of their simplicity and flexibility for modeling surfaces of arbitrary topology, subdivision surfaces have never been used for an apparently simpler problem—representing graph surfaces, *i.e.*, modeling smooth functions defined on planar domains. Instead, piecewise polynomial constructions like the Clough-Tocher and Powell-Sabin interpolants [15] are frequently used, splitting every triangle into multiple macro-triangles that may have bad aspect-ratios. Additionally, interpolation constraints may cause unwanted variations that are not present in surfaces defined by control points without interpolation, like B-Splines. Other approaches are based on multiquadrics [10, 11]. Some aspects of subdivision surfaces, however, have been exploited by a scattered-data fitting method based on triangular B-splines [22].

Classical visualization problems, like terrain modeling, have not taken advantage of subdivision techniques, in the past. In this paper we propose a simple and efficient variant of Loop's subdivision scheme [19, 26] for modeling scattered data in the plane. We expect that our subdivision technique will successfully be used for applications like terrain modeling and that trivariate constructions can be developed for volume modeling data defined on tetrahedral grids, as well.

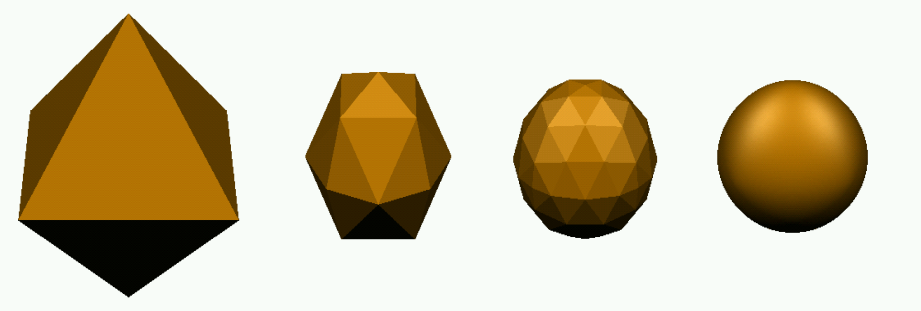

Fig. 1. Loop subdivision process. Starting with a triangulated control mesh (octahedron, left), a hierarchy of triangulations converges to a smooth limit surface (right).

2 Loop's Subdivision

We now review Loop's subdivision scheme [19] generalizng quartic box splines [15] to arbitrary triangular control meshes. The big deal about subdivision schemes is that they generate smooth surfaces from irregular control meshes with *extraordinary* points. Extraordinary points correspond to vertices that have other than four incident edges in a locally rectilinear mesh and vertices that have other than six incident edges in a triangle mesh. Thus, it is possible to define smooth surfaces of arbitrary topology by simple control meshes.

Starting with a triangulated control mesh, Loop's scheme splits every triangle into four by inserting a new vertex on every edge. This subdivision step is recursively repeated, resulting in a mesh hierarchy that converges to a smooth limit surface, see Figure 1. The coordinates of the control points are updated by linear, stationary subdivision rules, *i.e.*, the new points depend linearly on a local stencil of old control points and the masks for the updates are the same in every subdivision step.

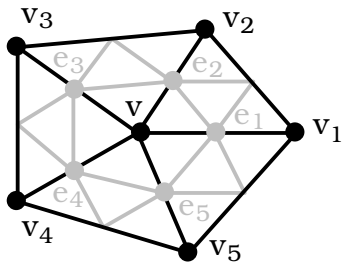

Fig. 2. Local indexing for the subdivision masks.

To explain the subdivision masks, we consider a particular vertex v with valence n (number of incident edges) and use a local indexing for the adjacent vertices v_i in some order ($i = 1, 2, \ldots, n$), see Figure 2. All indices are applied modulo n. The new vertices located on triangle edges are denoted by e_i. The first subdivision mask defines these vertices as

$$e_i \;=\; \frac{1}{8}(3v \;+\; 3v_i \;+\; v_{i-1} \;+\; v_{i+1}). \tag{2.1}$$

The second mask then updates the old vertices

$$\begin{aligned} v' \;&= \alpha_n v + (1-\alpha_n)\overline{v}, \quad \text{where} \\ \overline{v} \;&=\; \frac{1}{n}\sum_{i=1}^{n} v_i \quad \text{and} \\ \alpha_n \;&=\; \frac{3}{8} \;+\; \left(\frac{3}{8} \;+\; \frac{1}{4}\,cos\frac{2\pi}{n}\right)^2. \end{aligned} \tag{2.2}$$

Splitting every triangle into four and applying these two masks results in a finer mesh that is further subdivided using the same rules again and again.

Alternatively to the second mask we can update the old vertices v without duplicating their coordinates. Therefore, we replace equation (2.2) by the equivalent mask

$$\begin{aligned} v' \;&= (1-\beta_n)v + \beta_n\overline{e}, \quad \text{where} \\ \overline{e} \;&=\; \frac{1}{n}\sum_{i=1}^{n} e_i \quad \text{and} \\ \beta_n \;&=\; \frac{8}{5}(1-\alpha_n). \end{aligned} \tag{2.3}$$

In the case of a regular triangulation (without extraordinary points) using $\alpha_6 = \frac{5}{8}$, Loop's scheme reproduces quartic box splines. The choice of weights α_n ($n \geq 3$) implies C^1-continuity of the limit surface at extraordinary points [19]. The limit behavior of subdivision surfaces at extraordinary points can be computed from the eigenstructure of a local subdivision matrix, which first was done by Doo/Sabin [9]. This eigen-structure can be used to compute local control points of polynomial patches, resulting in an efficient algorithm for computing a subdivision surface and its partial derivatives at arbitrary parameter values [25].

3 Recursively Generated Graph Surfaces

We now consider the problem of constructing smooth graph surfaces $f(x, y)$ for triangulated scattered data in the plane. We start with a set of planar points $v_i = (x_i, y_i)$ ($i = 1, 2, \ldots, m$) with associated function values v_i^f and a triangulation Δ of these points. When applying Loop's subdivision to the triangulated mesh with control points (v_i, v_i^f), the planar triangulation is deformed by piecewise quartic polynomials, see Figure 3. Evaluating the surface at an arbitrary point (x, y) would be difficult since we would have to estimate corresponding local parameters in a certain triangle. Hence, we need to subdivide the triangles linearly and use Loop's scheme only for computing the function values. This, however, results in creases at the edges of Δ, see Figure 4. Only in the case of a regular triangulation with congruent triangles Loop's subdivision coincides with linear subdivision in the plane, due to linear precision, and a smooth graph surface is generated.

We want to modify the masks for Loop's subdivision in equations (2.1) and (2.3) such that they smooth out creases caused by the parametrization. Therefore, these masks must take into account the shapes of adjacent triangles. Only if these triangles are congruent, then the new masks should coincide with Loop's.

We use the same indexing as in equations (2.1) and (2.3), see Figure 5. First, we define the mask for the ordinates e_i^f at the new points e_i that are now midpoints of the corresponding edges. Therefore, we compute a parametric least-squares plane $\pi(x, y)$ [5] satisfying

$$3\left(\pi(v) - v^f\right)^2 + 3\left(\pi(v_i) - v_i^f\right)^2 + \left(\pi(v_{i-1}) - v_{i-1}^f\right)^2 + \left(\pi(v_{i+1}) - v_{i+1}^f\right)^2 \longrightarrow min. \tag{3.1}$$

This plane, evaluated at e_i, provides the new ordinate e_i^f.

As we will show in the following, this mask is linear, stationary, and reproduces equation (2.1) if both triangles are congruent, *i.e.*, if the vectors $v_{i+1} - v$ and $v_i - v_{i-1}$

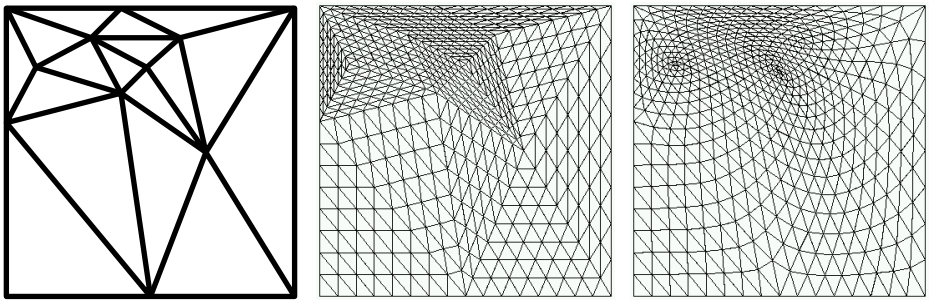

Fig. 3. Parametrizations for subdivision process. a) initial triangulation; b) linear subdivision; c) Loop subdivision deforming the triangles (boundary points are fixed).

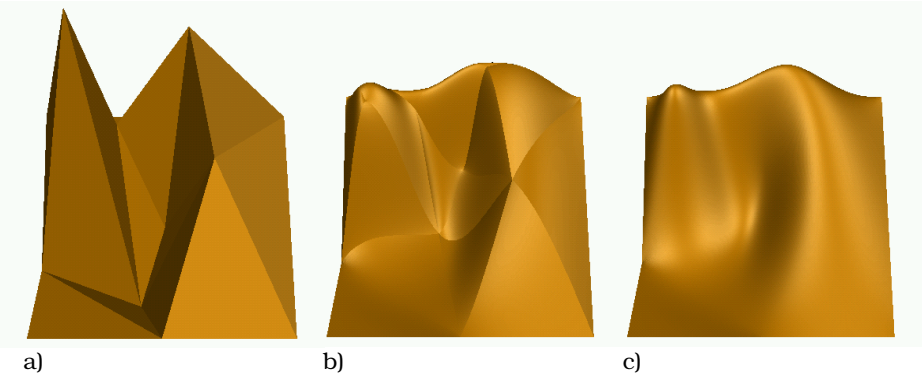

Fig. 4. Effect of parametrizations. a) initial control mesh based on the triangulation shown in Figure 3.; b) Loop's subdivision applied to ordinates causing creases at triangle edges; c) Loop's subdivision applied to all coordinates generating a smooth graph surface with deformed domain.

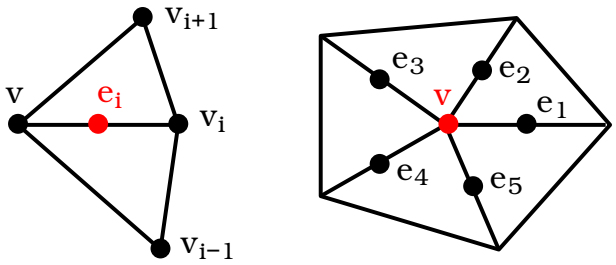

Fig. 5. Defining subdivision masks for the ordinates of e_i and v.

are equal. The plane π can be defined as

$$\begin{aligned} \pi(x,y) &= \sum_{i=1}^{3} c_i f_i(x,y), \quad \text{where} \\ f_0(x,y) &= 1, \\ f_1(x,y) &= x, \quad \text{and} \\ f_2(x,y) &= y. \end{aligned} \tag{3.2}$$

The coefficients c_i can be computed from a 3×3-system of equations

$$\begin{aligned} \mathbf{Ac} &= \mathbf{b}, \quad \text{where} \\ a_{kj} &= 3f_k(v)f_j(v) + 3f_k(v_i)f_j(v_i) \\ &\quad + f_k(v_{i-1})f_j(v_{i-1}) + f_k(v_{i+1})f_j(v_{i+1}), \quad \text{and} \\ b_k &= 3v^f f_k(v) + 3v_i^f f_k(v_i) + v_{i-1}^f f_k(v_{i-1}) + v_{i+1}^f f_k(v_{i+1}). \end{aligned} \tag{3.3}$$

For simplicity we chose a coordinate system with origin at e_i and the first mask becomes

$$e_i^f = c_0 = \tilde{\mathbf{a}} \cdot \mathbf{b} \tag{3.4}$$

where $\tilde{\mathbf{a}}$ is the first row of $\mathbf{A}^{-1}$, which always exists, since the four points v, v_i, v_{i-1} and v_{i+1} can only be collinear in a degenerate triangulation.

This mask is linear and invariant under affine transforms in the planar domain. In the special case of two equilateral triangles, the matrix A is diagonal and the mask becomes $\frac{1}{8}b_0$ which is the same as for Loop's subdivision. This result remains valid, if both triangles are congruent, due to affine invariance.

Analogously, we generalize the second mask of Loop's scheme, equation (2.3), by fitting a least-squares plane π. The ordinate v^f for a point v with valence n is updated by computing π, such that

$$(1-\beta_n)\left(\pi(v) - v^f\right)^2 + \beta_n \frac{1}{n} \sum_{i=1}^{n} \left(\pi(e_i) - e_i^f\right)^2 \longrightarrow min, \tag{3.5}$$

and by evaluating this plane at the point v. Again, we construct a system of equations for the coefficients c_i, as defined in equation (3.2):

$$\begin{aligned} \mathbf{Ac} &= \mathbf{b}, \quad \text{where} \\ a_{kj} &= (1-\beta_n)f_k(v)f_j(v) + \beta_n \frac{1}{n} \sum_{i=1}^{n} f_k(e_i)f_j(e_i), \quad \text{and} \\ b_k &= (1-\beta_n)v^f f_k(v) + \beta_n \frac{1}{n} \sum_{i=1}^{n} e_i^f f_k(e_i). \end{aligned} \tag{3.6}$$

This system is solved analogously to the system for the first mask. The same arguments hold for linearity, affine invariance, and existence of the solution. This second mask

reproduces Loop's scheme only for a vertex v surrounded by six congruent triangles, *i.e.*, by triangles resulting from equilaterals when applying an affine map.

We note that these masks can be pre-computed. Due to affine invariance, there is at most one different mask for every vertex and for every edge of the initial triangulation Δ. Thus, our scheme is stationary. All vertices generated on the same edge of Δ use the same mask. For the majority of newly generated vertices that are not located on an edge or vertex of the initial triangulation Δ, we can apply Loop's subdivision rules directly to compute the corresponding ordinates.

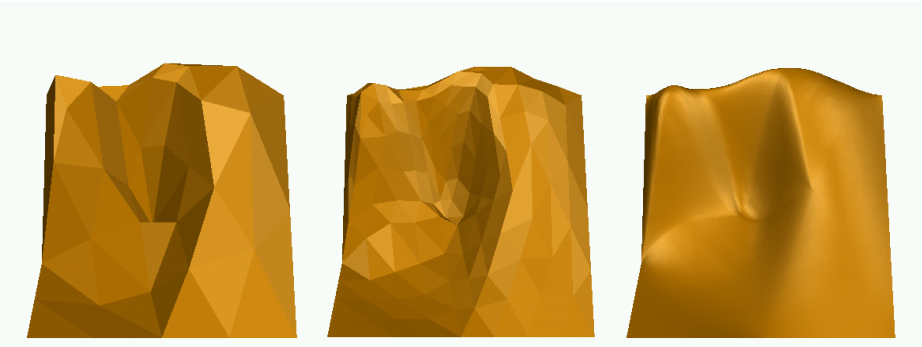

Fig. 6. Subdivision process and limit surface for our subdivision scheme. a) first subdivision level; b) second level; c) resulting surface (sixth level).

4 Results and Future Work

Our linear, stationary subdivision scheme provides the following properties:

- It is invariant under affine transforms in the plane.
- It has linear precision.
- Our scheme generates piecewise polynomial surfaces.
- It coincides with Loop's subdivision and with quartic box-splines on a regular grid composed of congruent triangles.

Surface regions that are strictly located inside the triangles of Δ are eventually determined by Loop's subdivision rules, after applying a finite number of subdivision steps. This implies that our subdivision surfaces are composed of quartic patches and are C^1-continuous in all points strictly inside the individual triangles of Δ. For the remaining points a rigorous mathematical analysis of the limit-behavior considering the eigen-structure of local subdivision matrices needs still to be done.

The subdivision process for a surface generated with our scheme using a control mesh (Figure 4a.) composed of 13 vertices and 17 triangles is shown in Figure 6. This surface appears to be much smoother than the one generated with Loop's subdivision

masks applied to the ordinates, shown in Figure 4b. However, it does not look as fair as the surface generated by Loop's subdivision applied to all coordinates, see Figure 4c. This is due to the constraints for the parametrization that do not allow the surface to relax parallel to the plane. These constraints are useful, however, since they lead to limit surfaces that better preserve the shape of the initial control mesh. Additionally, these constraints imply that the vertices of the initial triangulation Δ are fixed in the plane. Thus, we can easily interpolate certain ordinates at these vertices by solving for the corresponding control points. Interpolating normals and surface fairing can also be accomplished with subdivision surfaces [14, 16].

Figure 7. shows our subdivision scheme applied to the triangulated terrain model "Crater Lake", composed of 9890 vertices and 19380 triangles, courtesy of U.S. Geological Survey. To obtain a mesh that is irregular in nature, we have simplified the triangulation to a resolution of 5000 triangles by collapsing edges. Our subdivision scheme significantly increases the quality of rendered images when compared to a Gouraud-shaded triangulation, see Figure 7.

We note that all levels of resolution obtained by subdivision represent the same geometric information. It is possible to introduce additional surface detail at every subdivision level by locally perturbing the control points of the subdivided meshes. These perturbations can compactly be represented by wavelet coefficients, providing a sparse and highly efficient multiresolution surface representation [20].

In this paper we have motivated the use of subdivision surfaces for scattered data approximation and presented a new subdivision scheme. We have demonstrated that our method is well suited for terrain modeling. It is also possible to use our subdivision scheme for approximating bivariate functions with multi-dimensional ranges, like planar tensor fields and color images. Future work will be directed at the construction of trivariate subdivision schemes for volume modeling. Additionally, we want to improve the fairness of our functional subdivision surfaces by incorporating variational principles [13, 16] into our subdivision scheme.

References

1. M. Bertram, *Multiresolution Modeling for Scientific Visualization*, Ph.D. Thesis, University of California at Davis, July 2000.
   `http://graphics.cs.ucdavis.edu/~bertram`
2. M. Bertram, M.A. Duchaineau, B. Hamann, and K.I. Joy, *Wavelets on planar tesselations*, Proceedings of the International Conference on Imaging Science, Systems, and Technology, CSREA Press, 2000, pp. 619–625.
3. M. Bertram, M.A. Duchaineau, B. Hamann, and K.I. Joy, *Bicubic subdivision-surface wavelets for large-scale isosurface representation and visualization*, Proceedings of IEEE Visualization 2000, pp. 389–396 & 579.
4. H. Biermann, A. Levin, and D. Zorin, *Piecewise smooth division surfaces with normal control*, Proceedings of ACM Siggraph 2000, pp. 113–120.
5. W. Boehm and H. Prautzsch, *Geometric Concepts for Geometric Design*, A.K. Peters, Ltd., Wellesley, Massachusetts, 1994.
6. G.-P. Bonneau, *Optimal triangular Haar bases for spherical data*, Proceedings of IEEE Visualization 1999, pp. 279–284 & 534.

7. E. Catmull and J. Clark, *Recursively generated B-spline surfaces on arbitrary topological meshes*, Computer-Aided Design, Vol. 10, No. 6, 1978, pp. 350–355.
8. T. DeRose, M. Kass, and T. Truong, *Subdivision surfaces in character animation*, Proceedings of ACM Siggraph 1998, pp. 85–94.
9. D. Doo and M. Sabin, *Behaviour of recursive division surfaces near extraordinary points*, Computer-Aided Design, Vol. 10, No. 6, 1978, pp. 356–360.
10. R. Franke and H. Hagen, *Least squares surface approximation using multiquadrics and parametric domain distortion*, Computer-Aided Geometric Design, Vol. 16, No. 3, Elsevier, 1999, pp.177–196.
11. R. Franke, H. Hagen, and G. Nielson, *Repeated knots in least squares multiquadric functions*, Computing Supplement 10, Geometric Modelling, Springer, 1995, pp. 177–187.
12. I. Guskov, W. Sweldens, and P. Schröder, *Multiresolution signal processing for meshes*, Proceedings of ACM Siggraph 1999, pp. 325–334.
13. H. Hagen, G. Brunnett, and P. Santarelli, *Variational principles in curve and surface design*, Surveys on Mathematics for Industry, Vol. 3, No. 1, 1993, pp. 1–27.
14. M. Halstead, M. Kass, and T. DeRose, *Efficient, fair interpolation using Catmull-Clark surfaces*, Proceedings of ACM Siggraph 1993, pp. 35–44.
15. J. Hoscheck and D. Lasser, *Fundamentals of Computer Aided Geometric Design*, A.K. Peters, 1993.
16. L. Kobbelt, *Discrete fairing and variational subdivision for freeform surface design*, Visual Computer, Vol. 16, No. 3–4, Springer, 2000, pp. 142–158.
17. L. Kobbelt, J. Vorsatz, and H.-P. Seidel, *Multiresolution hierarchies on unstructured triangle meshes*, Computational Geometry: Theory and Applications, Vol. 14, No. 1-3, Elsevier, 1999, pp. 5–24.
18. L. Kobbelt and P. Schröder, *A multiresolution framework for variational subdivision*, ACM Transactions on Graphics, Vol. 17, No. 4, 1998. pp. 209–237.
19. C.T. Loop, *Smooth subdivision surfaces based on triangles*, M.S. Thesis, Department of Mathematics, University of Utah, 1987.
20. M. Lounsbery, T. DeRose, and J. Warren, *Multiresolution analysis for surfaces of arbitrary topological type*, ACM Transactions on Graphics, Vol. 16, No. 1, 1997, pp. 34–73.
21. G.M. Nielson, I.-H. Jung, and J. Sung, *Haar wavelets over triangular domains with applications to multiresolution models for flow over a sphere*, Proceedings of IEEE Visualization 1997, pp. 143–150.
22. R. Pfeifle, H.-P. Seidel, *Fitting triangular B-splines to functional scattered data*, Computer Graphics Forum, Vol. 15, No. 1, Backwell Publishers, 1996, pp. 15–23.
23. U. Reif, *A unified approach to subdivision algorithms near extraordinary vertices*, Computer-Aided Geometric Design, Vol. 12, No. 2, 1995, pp.153–174.
24. P. Schröder and W. Sweldens, *Spherical wavelets: efficiently representing functions on the sphere*, Proceedings of ACM Siggraph 1995, pp. 161–172.
25. J. Stam, *Exact evaluation of Catmull-Clark subdivision surfaces at arbitrary parameter values*, Proceedings of ACM Siggraph 1998, pp. 395–404.
26. E.J. Stollnitz, T.D. DeRose, D.H. Salesin, *Wavelets for Computer Graphics—Theory and Applications*, Morgan Kaufmann, 1996.
27. H. Weimer and J. Warren, *Subdivision schemes for fluid flow*, Proceedings of ACM Siggraph 1999, pp. 111–120.

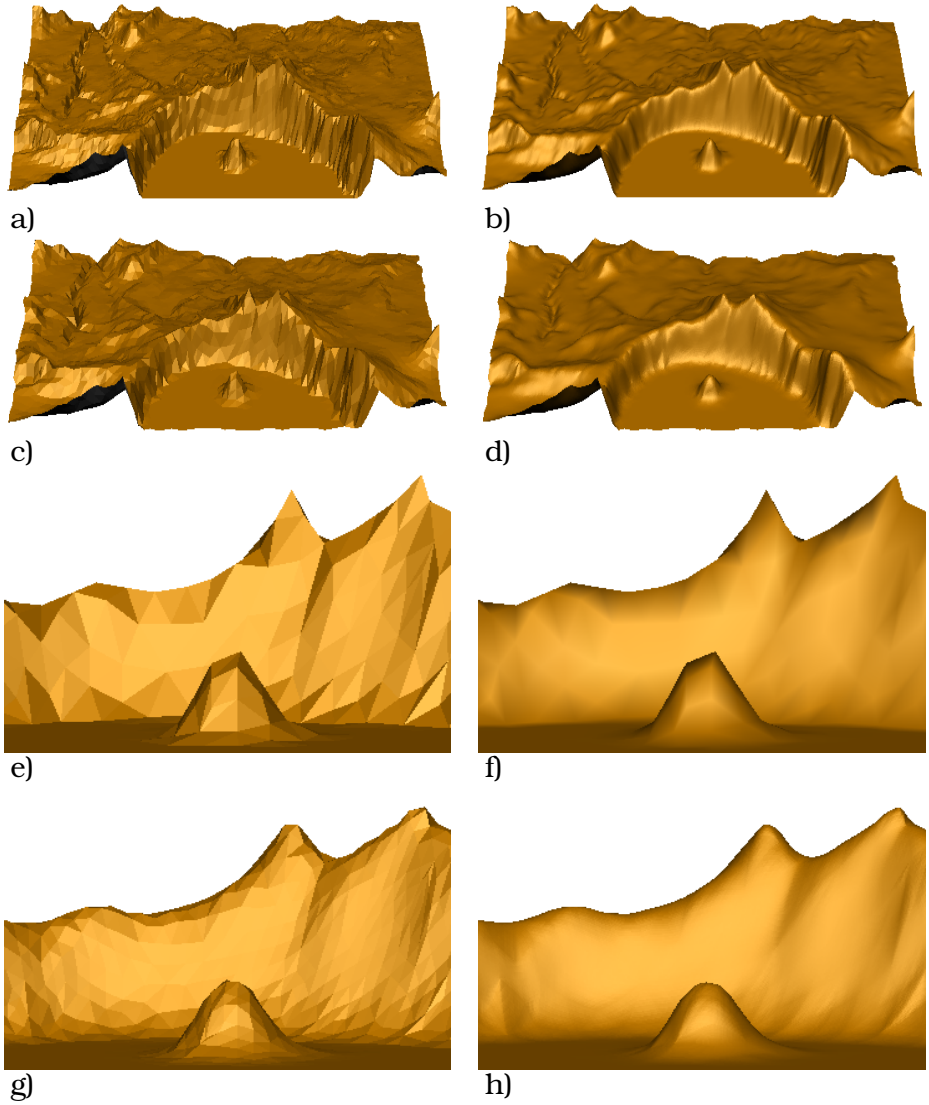

Fig. 7. Modified Loop subdivision for “Crater-Lake” terrain model. a) Original model (19380 triangles); b) third subdivision (1240320 triangles); c) simplified model (5000 triangles); d) third subdivision (320000 triangles); e) local view of c); f) Gouraud shaded; g) first subdivision; h) fourth subdivision.